USE OF TRACERS FOR THE CHARACTERIZATION OF SCALE-DEPENDENT SUBSURFACE PROCESSES: INITIAL EVALUATION

G.R. Barth, T.H. Illangasekare, and H. Rajaram, Department of Civil and Environmental Engineering, University of Colorado at Boulder, Boulder, CO, 80309-0428, Phone: 303-492-6754, FAX: 303-492-7317

ABSTRACT Determination of the distribution and quantity of non-aqueous phase liquids (NAPL) in the subsurface requires accurate evaluation of the effective parameters governing flow in porous media. A great deal of the work done towards the development of effective parameters has focused on analysis techniques for adapting parameters determined from a small-scale to a field-scale system. These techniques suffer from the inherent limitations of developing conclusions about regional or grid-scale flow based on a limited number of smaller-scale, isolated measurements. A conservative tracer injected into heterogeneous media will, however, be affected by all the heterogeneities encountered in the existing flow-fields between the site of injection and extraction. A tracer test provides a direct measurement of the heterogeneous system. A series of tracer tests were performed to assess the ability of tracers to function as a tool for determining effective field-scale parameters. Experimental design focused on creating a heterogeneous system with known stochastic parameters which could be modified by NAPL entrapment. The analytical work concentrated on developing techniques to interpret the tracer test results.

KEY WORDS: effective parameter, tracer, scaling

INTRODUCTION

The remediation of aquifers contaminated with organic chemicals is a topic of public concern as well as a considerable scientific and engineering challenge. Of particular concern are chemicals and waste products in the form of non-aqueous phase liquids (NAPL). Some of the more common NAPLs include industrial solvents, sludges, and petroleum refinery byproducts. NAPLs are typically released into the environment from leaking underground storage tanks, pipelines, and accidental spills. Denser-than-water NAPLs such as creosote, TCA, TCE, and PCB are particularly troublesome when released into the environment due to their complex behavior in naturally heterogeneous subsurface systems. NAPLs have the potential to become entrapped in a variety of ways, resulting in a wide range of possible spatial distributions. For example, micro-scale entrapment produces a relatively uniform distribution of residual saturation while macro-scale entrapment produces pockets of contamination distributed randomly as a function of the distribution of subsurface heterogeneities. Even the manner of residual saturation can vary, ranging from thin coatings on individual grains to extruded ganglia extending multiple pore lengths. Regardless of the mechanism, entrapped NAPLs have the potential to act as long-term sources of contamination in ground water because they experience limited dissolution. When the solubility limit of the NAPL exceeds water quality standards, the entrapped NAPL serves as a source of significant contamination. If left untreated, the persistence of the NAPL provides a long term source of ground water contamination

through leaching of the more soluble components.

In order to effectively remediate a site, techniques are required to determine the spatial distribution of entrapped contaminants and the degree of saturation. Current techniques typically rely on data which is obtained by core-scale sampling. Sampling on the core scale typically results in data from a scale much smaller than the scale of the heterogeneities in the field. In order to capture variability due to natural systems, a method of measurement capable of evaluating at the field scale must be employed. It is our hypothesis that tracer tests are one of the few methods capable of actually measuring the changes in constitutive parameters at the field scale before and after a spill. The shape of the breakthrough curve (BTC) is a function of the effective field-scale parameters. We hypothesize that NAPLs entrapped in the subsurface will change these parameters and result in a different BTC. The impact of the entrapped NAPL on the shape of the BTC has the potential to indicate the stochastic parameters of the entrapped distribution. To evaluate the potential of this method of characterization, a series of experiments were performed in a tank with a known stochastic, heterogeneous distribution of materials. The experiments consisted of a series of tracer tests to produce BTCs for conditions prior to a spill, after a spill, and after remediation. The results give a preliminary indication of the potential of this technique.

THEORY

The transport of tracers by ground water is governed by the combination of advective and dispersive processes. Equation 1 is the one-dimensional form of the advection-dispersion equation for non-reactive dissolved constituents in saturated, homogeneous, isotropic materials under steady uniform flow. In Equation 1, C is the concentration of solute, l is the curvilinear coordinate direction taken along the flow-line, $\bar{v}$ is the average linear ground water velocity, t is time and D_l is the coefficient of hydrodynamic dispersion in the longitudinal direction. The coefficient of hydrodynamic dispersion can be expressed in terms of two components, where α_l is the dispersivity and D^* is the coefficient of molecular diffusion. For most applications of transport in ground water, the diffusion term is ignored because the dispersive forces dominate. Diffusion is included only under conditions of very low flow rates; when the impact of the dispersivity term becomes less significant.

$$D_l \frac{\partial^2 C}{dl^2} - \bar{v}_l \frac{\partial C}{\partial l} = \frac{\partial C}{\partial t} \quad (1)$$

$$D_l = \alpha_l \bar{v} + D^* \quad (2)$$

Although there has been extensive work characterizing both velocity and dispersivity in heterogeneous systems, dispersivity is far less well understood. Dispersivity is a fundamental characteristic property of the porous medium and has been shown to be a function of the grain size and grain size distribution. Typically, measurements of dispersivity are performed in the laboratory on small cores extracted from the field site. Unfortunately the values of dispersivity observed in the field are typically several orders of magnitude larger than the values obtained in the laboratory [1, 2]. This phenomena is typically referred to as scaling: a parameter measured on one scale will be orders of magnitude different than when measured on a different scale. In order to address the issue of scaling, it is necessary to measure the dispersivity of a system on the scale at which it will be applied. At the core scale, evaluating primarily

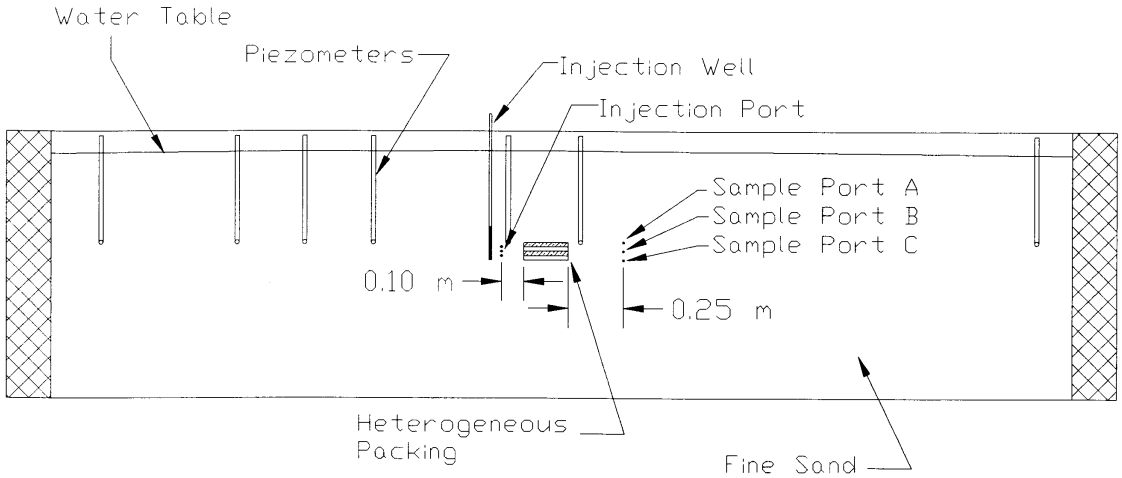

FIGURE 1. LARGE TANK WITH SIMPLE HETEROGENEOUS PACKING.

homogeneous material, dispersivity behaves according to its definition. The tortuous paths which the flow must traverse impose mixing and differential velocities on the liquid. The differences in velocity cause the characteristic spreading of the solute front which is parameterized as dispersivity. On the field scale the dominant force causing differences in velocities of the flow field is not the tortuosity of the flow paths at the grain scale, but the variations in flow due to transitions between large-scale heterogeneities. The effect of variations in hydraulic conductivity on field-scale dispersion is documented in theoretical [3, 4] and field studies [5, 6]. The end result is much more spreading of tracer fronts in the field than that predicted by laboratory measurements. For this reason the dispersivity measured at field scale is commonly referred to as the effective or macro-scale dispersivity.

For a given realization from a stochastic distribution of sub-surface properties there will be a distinct BTC. Not that there is a unique BTC for each configuration of the subsurface, but rather that statistical properties of the subsurface parameters can be determined according to the dispersivity observed. The statistical properties are impacted by contaminants entrapped in the subsurface, especially in the case of NAPLs with their high potential for macro-scale entrapment in heterogeneous formations. Changes in the observed BTC due to entrapped contaminants have the potential to indicate their quantity and spatial distribution in the subsurface.

PROCEDURES

Porous medium

A series of laboratory experiments were conducted to evaluate the potential of tracer tests for determining dispersivity of a heterogeneous system. A large two-dimensional tank was filled with a heterogeneous packing of different sands (Figure 1). A crushed and sieved silica sand, free from organic matter and clays, with the trade name Unimen Silica was used to create the heterogeneous formation. As many as five different sizes, classified as very coarse (No. 8), coarse (No. 16), medium (No. 30), fine (No. 70), and very fine (No. 110) were used. All the sizes were found to be very uniform based on sieve analysis. Table 1

summarizes the sand parameters. The soil grain size distribution data was obtained using ASTM C136, moisture characteristics were determined by the flow pump method of Znidarcic, *et al.* [7], and hydraulic conductivity was measured using the constant head method [8].

Heterogeneous formation in a large tank

For the first series of experiments a heterogeneous aquifer was simulated in two dimensions by packing five different sands into a section of a 9.8 meter long tank. The test section of the tank was 0.05 meters thick, 4.8 meters long, and 1.2 meters high. Sand was placed in the tank in a rectangular configuration consisting of 50 rows and 22 columns. Each of the 1,100 cells measured 20 cm long, two cm tall, and five cm across. With the resemblance to real-world heterogeneous systems in mind, an anisotropy ratio of 1:10 (ratio of vertical to horizontal correlation scales of ln K) was selected. With a total horizontal length of 4.8 m in the tank, a horizontal block size of 20 cm and horizontal correlation scale of 40 cm was used. The vertical correlation scale was 4.0 cm, with a block size of 2 cm. The grid resolution was one-half of a correlation scale in each direction. A realization of a random field was generated using a Fourier summation algorithm with the correlation scales mentioned above. The sand with the value of ln K closest to the generated value was assigned to that grid cell.

After testing the tank for leaks, a one cm layer of clay was placed in the bottom to act as an impermeable layer. On top of the clay, nine cm of #30 mesh silica sand (d50 = 0.48 mm) was packed in two cm lifts. The next 100 cm of depth was dry packed in two cm by 20 cm long cells according to the random field discussed above. An additional two cm of # 30 sand was then packed on top to allow the heterogeneous configuration to remain undisturbed. Finally, the water table was raised over a period of days using constant head devices connected to the ends of the tank. A variety of tracer injection and sampling port configurations were evaluated.

The second series of tests focused on a simpler configuration. This configuration simulated a two-dimensional, heterogeneous aquifer in which the effective dispersivity was significantly different from the grain scale dispersivity. The data analyzed in this report originated from the second series of experiments. The tracer injection port for the experiments was located 0.15 m up-gradient of the heterogeneity and centered vertically with the heterogeneity. The sampling ports were located 0.25 m down-gradient of the heterogeneities (Figure 1). To determine an optimal sampling interval, a food dye was injected into the media and the qualitative progress monitored through the tank. This allowed the sampling interval to be adjusted to higher frequencies as needed to capture the BTC without maintaining a high sampling rate for the entire experiment.

TABLE 1. SAND PARAMETERS.

Sand Type	#8	#16	#30	#70	#110
K_w (cm/s)	1.20	0.43	0.15	0.02	0.004
d_{50}	1.50	0.88	0.49	0.19	0.103
d_{60}/d_{10}	1.39	1.72	1.50	1.86	not available

Light non-aqueous phase liquid

A low-toxicity, nonvolatile, light-industrial organic solvent with the trade name Soltrol 220 (Phillips Petroleum Inc., Bartleville, Okla.), was selected as the lighter-than-water NAPL for these experiments. Soltrol 220 was selected based on its low toxicity, favorable attenuation characteristics, and relative cost. The Soltrol 220, which is a clear fluid, was colored with an inert red organic dye to create a visual contrast so that the plume configurations could be easily observed. Table 2 lists fluid properties.

Potassium Bromide tracer

Potassium Bromide (KBr) was selected as the tracer due to its conservative, non-reactive characteristics and its extensive use in field applications. Concentrations of 10^{-2} M KBr were injected into the heterogeneous medium and sampled at a series of down-gradient ports. All samples were analyzed using an Orion 9435 ion selective Bromide probe in conjunction with a 90200 dual junction reference electrode. The probes were read with an Orion 545A pH/millivolt meter. Values of voltage were converted to pH by determining the concentration/voltage relation from a series of standard solutions.

Analysis

In order to analyze the BTC data, the observed values were compared to modeled values. The model consisted of the equation for two-dimensional advection-dispersion of a conservative solute in a uniform, saturated ground water flow field, ignoring the diffusion component of hydrodynamic dispersion (Equation 3). The terms α_x and α_y represent the dispersivity in the x and y directions respectively. Flow velocity is designated by $\bar{v}$.

$$\bar{v}\alpha_x \frac{\partial^2 C}{\partial x^2} + \bar{v}\alpha_y \frac{\partial^2 C}{\partial y^2} = \frac{\partial C}{\partial t} + \bar{v}\frac{\partial C}{\partial x} \tag{3}$$

For certain boundary conditions and assumptions, Equation 3 can be solved for the concentration as a function of location and time. Equation 4 is the solution to Equation 3 for the instantaneous input of a mass, M, of solute as a vertical line source at x, y, and t = 0, in a uniform infinite flow field resulting in a two-dimensional plume. In Equation 4, *b* is the thickness, and *n* is the porosity. To determine the values of α_x and α_y, Equation 4 can be solved inversely using measured values of concentration at a specific location. Unfortunately, Equation 4 is a non-linear relation. To perform the inversion, a model-independent parameter estimation routine, PEST, was used [9]. To implement PEST, a short FORTRAN program was written to calculate Equation 4. The program read an input data file consisting of values for α_x, α_y, $\bar{v}$, and *C*. The input file had one value for α_x, α_y, and $\bar{v}$ (the model parameters) and a time series of values for *C*. By creating a series of instruction files, PEST was able to link with "dsp.for," running the program repeatedly and evaluating the shape of the BTC until

TABLE 2. FLUID PROPERTIES (AT 25ºC).

Fluid	Density (g/cc)	Viscosity (cP)	σ w/H_20 (dyne/cm)	σ w/air (dyne/cm)
H_20	1.000	1.12	N/A	27
Soltrol	0.789	6.12	42	71

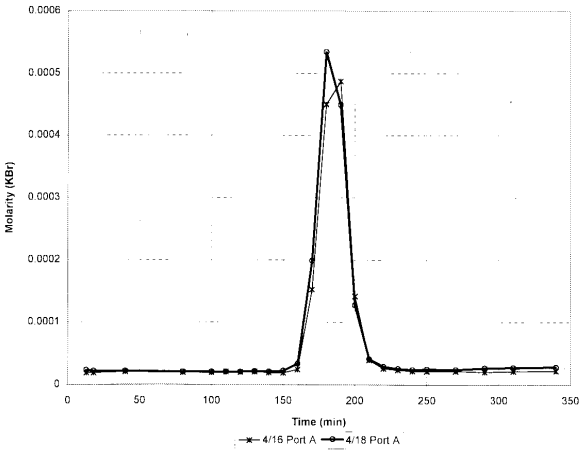

FIGURE 2. REPEATABILITY OF BREAKTHROUGH CURVES: PORT A.

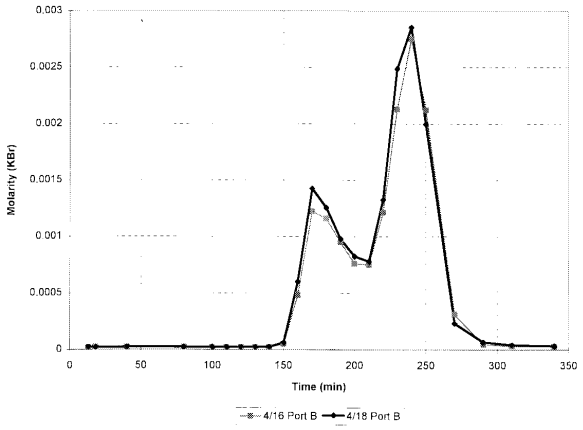

FIGURE 3. REPEATABILITY OF BREAKTHROUGH CURVES: PORT B.

the fit was optimized.

$$C(x,y,t) = \frac{M}{4\pi t\bar{v}bn\sqrt{(\alpha_x\alpha_y)}} e^{\left[-\frac{(x-\bar{v}t)^2}{4\bar{v}\alpha_x t} - \frac{y^2}{4\bar{v}\alpha_y t}\right]} \quad (4)$$

RESULTS

Due to initial problems with the KBr probe, the data from the first set of experiments is not presented in this paper. The analysis performed and the results presented are a product of the second series of experiments.

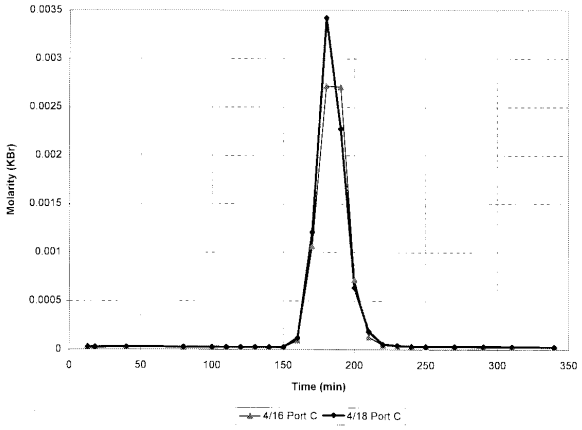

FIGURE 4. REPEATABILITY OF BREAKTHROUGH CURVES: PORT C.

Figures 2-4 demonstrate the repeatability of results for the experiments. The BTCs depict the arrival of the KBr tracer, which was injected into the port up-gradient of the heterogeneity, at the sampling ports down-gradient of the heterogeneity (Figure 1). The impact of the heterogeneity was especially distinct in Figure 3, which detected a peak traveling through both the fine grain and coarse grain material. The impact of the entrapped NAPL is evident in Figures 5-7. The three figures show the BTC for each of the ports before the spill, after the spill, and after flushing with surfactant as a method of remediation. A clear trend of impact is present for each of the curves. The peak of the BTC was delayed by the spill as compared with the pre-spill BTC, while the post-remediation BTCs rebounded back toward the pre-spill shape.

Analysis for effective parameters from the individual port's BTCs produced fairly erratic results with only minimal trends in the dispersivity as a function of entrapped contaminant and remediation. Even with optimized coefficients which were well beyond any reasonable values the BTCs generated by Equation 4 were unable to match the observed BTCs. The generated

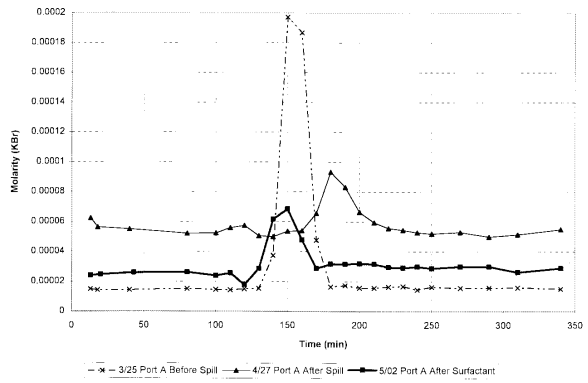

FIGURE 5. PORT A BREAKTHROUGH CURVES: BEFORE SPILL, AFTER SPILL, AND AFTER SURFACTANT FLUSHING.

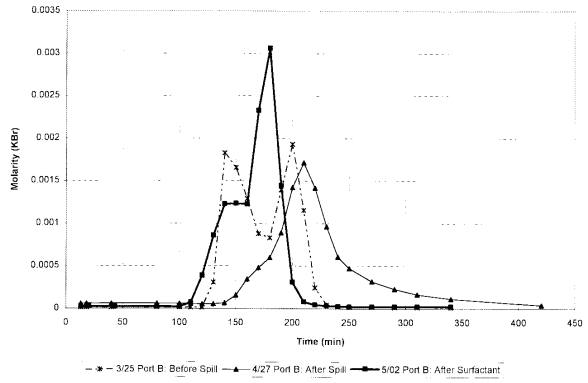

FIGURE 6. PORT B BREAKTHROUGH CURVES: BEFORE SPILL, AFTER SPILL, AND AFTER SURFACTANT FLUSHING.

BTCs consistently under-estimated the observed concentration. A one-dimensional solution was evaluated, but it consistently overestimated the values of concentration in the BTC. Finally, a quasi two-dimensional approach was evaluated. The two-dimensional solution was used (Equation 4), but the observed and fitted BTCs were averaged across the three ports. This provided a more stable data set against which the solution could be optimized. Figure 8 demonstrates schematically the potential for improvement using this approach. The individual values at each port differ significantly from the predicted solution, but the average value from the

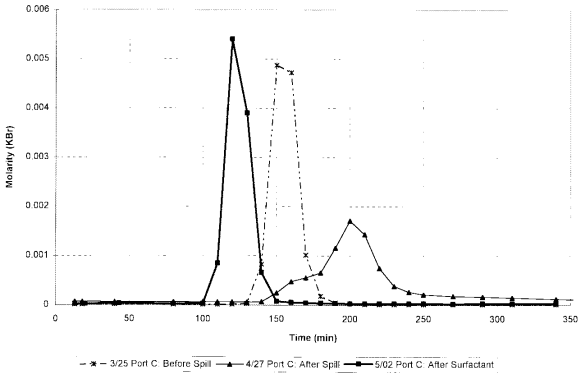

FIGURE 7. PORT C BREAKTHROUGH CURVES: BEFORE SPILL, AFTER SPILL, AND AFTER SURFACTANT FLUSHING.

observed data is very close to the average of the predicted. Table 3 lists the values of effective velocity and effective longitudinal and transverse dispersivity according to Equation 4 and the average BTCs. In this context the effective velocity simply reflects the time for the BTC peak to arrive at the sampling ports. In addition to being more reasonable than the values generated from fitting Equation 4 to the individual ports, the values in Table 3 exhibited reasonable trends (Figure 9). The spill caused an increase in both the effective longitudinal and transverse dispersivities. In addition, that increase was almost reversed by the remediation efforts. Figure 9 also exhibits the same sort of trend for the effective velocity.

DISCUSSION

The values determined by this approach represent effective parameters. Their values may not be subject to the strict interpretation of their definitions, but they provide a practical method of evaluating subsurface entrapment on the spill scale. The values in Table 3 indicate a clear trend of entrapment and its impact on the flow regime. The results even suggest the potential for

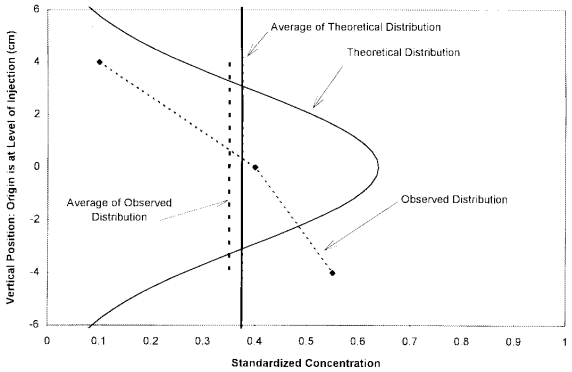

FIGURE 8. THEORETICAL AND OBSERVED VERTICAL DISTRIBUTION OF SOLUTE BREAKTHROUGH CURVE.

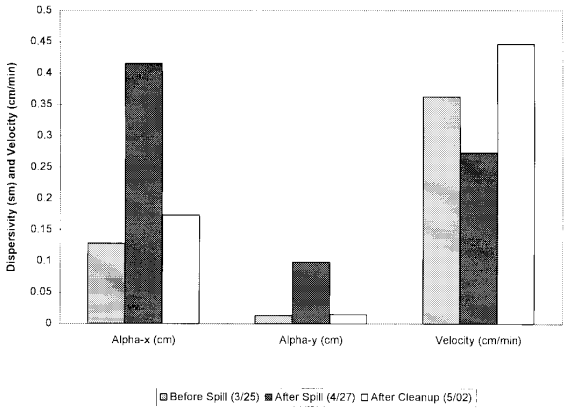

FIGURE 9. OPTIMIZED PARAMETERS USING BTC AVERAGING: BEFORE SPILL, AFTER SPILL, AND AFTER SURFACTANT FLUSHING.

evaluating the success of remediation efforts. The post-cleanup values of dispersivity did not return to their original pre-spill levels although in this case the difference was not significant.

The averaging of the BTCs from individual ports can be viewed as the same phenomena which would occur for a fully-screened sampling well. The inherent limitations of Equation 4, due to the assumptions involved, eliminates the possibility of interpreting the individual BTCs. However, the composite BTC, indicating an average concentration for the three ports at each time step, can be evaluated by Equation 4 to produce effective parameters.

The effective velocity behaved as expected due to the entrapped NAPL. The contaminant in the porous medium physically obstructed flow of the tracer, resulting in a later peak in the BTC which in turn is interpreted as a slower effective velocity. Interpretation of the post remediation velocity is a bit more specific. Prior to the spill the tracer progressed through both the fine material and the coarse material. During the spill both of these avenues were partially blocked, resulting in a later BTC as discussed above. Remediation of the spill resulted in a significant reduction of the entrapped NAPL. However, the residual NAPL remaining after the remediation had a greater impact on the flow through the fine-grain material. The result was a decreased

TABLE 3. VALUES OF EFFECTIVE VELOCITY AND EFFECTIVE LONGITUDINAL AND TRANSVERSE DISPERSIVITY ACCORDING TO EQUATION 4 AND THE AVERAGE BTCS.

Experiment	Effective Longitudinal Dispersivity (cm)	Effective Transverse Dispersivity (cm)	Effective Velocity (cm/min)
Before spill	0.128242	0.013531	0.362582
After spill	0.415218	0.098461	0.273079
After cleanup	0.173577	0.014932	0.445767

flow through the fine-grain material and a relative increase through the coarse-grain material, producing an earlier peak in the BTC and a faster effective velocity.

The values of effective longitudinal dispersivity determined with the tracers compare well with values determined by Szlag [10] using independent methods. In addition, the effective parameters responded to the spill and remediation as would be expected. For the #16 sand, Szlag obtained a value of 0.285 cm and a value of 0.070 cm for the #30 sand. These values can be compared to the effective values of 0.128, 0.415, and 0.174 cm from before the spill, after the spill, and after remediation, respectively. The effective values are of the same order of magnitude as the measured values because of the limited scale of the experiment. The value of effective dispersivity before the spill was the lowest (0.128 cm), after the spill it was the highest (0.415 cm), and after remediation it returned to almost pre-spill levels (0.174 cm). The agreement between the effective values and those measured by Szlag combined with the reasonable response to the spill and remediation helped demonstrate the potential of the technique.

CONCLUSIONS

This paper summarizes the efforts to combine detailed experiments with analytical methods. Just to perform the experiments required considerable effort to create conditions which would be analogous to real world situations. Evaluation of the data by the appropriate techniques demonstrated the potential of this approach to provide valuable information on the quantity and distribution of entrapped contaminants in the subsurface. The tracer test avoids the pitfalls of small-scale sampling and provides information on the scale of the spill. In order to proceed to a field-scale evaluation, additional work is required. However, even these limited experiments have demonstrated the ability of the tracer test to evaluate the significance of remediation efforts.

ACKNOWLEDGMENTS

The support of the U.S. EPA through the Great Plains/Rocky Mountain Hazardous Substance Research Center at Kansas State University and the U.S. Army Research Office at Research Triangle Park, North Carolina, is gratefully acknowledged. In addition the extensive laboratory work of J. Ewing and K. Pytte is also gratefully acknowledged.

Although this article has been funded in part by the U.S. Environmental Protection Agency under assistance agreement R-819653, through the Great Plains-Rocky Mountain Hazardous Substance Research Center, headquartered at Kansas State University, it has not been subjected to the agency's peer and administrative review and, therefore, may not necessarily reflect the views of the agency. No official endorsement should be inferred.

REFERENCES

1. L.W. Gelhar, C. Welty, and K.R. Rehfeldt, A critical review of data on field-scale dispersion in aquifers, Water Resources Research, 28:7 (1992) 1955-1974.

2. L.W. Gelhar, A. Montaglou, C. Welty, and K.R. Rehfeldt, A Review of Field-Scale Physical Solute Transport Processes in Saturated and Unsaturated Porous Media, EPRI Report EA-4190, Elec. Power Res. Inst., Palo Alto, CA, August, 1985.

3. L.W. Gelhar and C.L. Axness, Three-dimensional stochastic analysis of macrodispersion in aquifers, Water Resources Research, 19:1 (1983) 161-180.

4. G. Dagan, Solute transport in heterogeneous porous formations, Journal of Fluid Mechanics, 145 (1984) 151-177.

5. D.M. Mackay, D.L. Freyburg, P.V. Roberts, and J.A. Cherry, A natural gradient experiment on solute transport in a sand aquifer: 1. Approach and overview of plume movement, Water Resources Research, 22:13 (1986) 2017-2029.

6. D.R. LeBlanc, S.P. Garabedian, K.M. Hess, L.W. Gelhar, R.D. Quadri, K.G. Stollenwerk, and W.W. Wood, Large scale natural gradient tracer test in sand and gravel, Cape Cod, Massachusetts: 1. Experimental design and observed tracer movement, Water Resources Research, 27:5 (1991) 895-910.

7. D. Znidarcic, T.H. Illangasekare, and M. Manna, Laboratory testing and parameters estimation for two phase flow, Proc. ASCE Conf. in Geotech. Engrg., ASCE, NY, 1991, pp. 1078-1089.

8. R.A. Freeze and J.A. Cherry, Groundwater, Prentice-Hall Inc., Englewood Cliffs, NJ, 1979.

9. Watermark Computing, PEST, a model-independent parameter optimization, 1994.

10. D. Szlag, Dissolution of Trapped Waste Chemicals, Ph.D. Dissertation, University of Colorado, Boulder, Colorado, 1996.